For submission to *Neuropharmacology*

Neuroprotectant effects of iso-osmolar D-mannitol to prevent Pacific ciguatoxin-1 induced alterations in neuronal excitability: a comparison with other osmotic agents and free radical scavengers

Liesl C. Birinyi-Strachan[a], Michael J. Davies[b], Richard J. Lewis[c] and Graham M. Nicholson[a,*]

[a]Neurotoxin Research Group, Department of Health Sciences, University of Technology, Sydney, Broadway NSW, Australia

[b]The Heart Research Institute, Camperdown NSW, Australia

[c]Institute for Molecular Bioscience, University of Queensland, Brisbane, QLD 4072 Australia

Running Title: Neuroprotectant effects of D-mannitol in ciguatera

Keywords: ciguatoxin; sodium channels; D-mannitol; Trolox; L-ascorbic acid; D-sorbitol

Corresponding author: Associate Professor Graham M. Nicholson
Department of Health Sciences
University of Technology, Sydney
P.O. Box 123
Broadway NSW 2007
Australia

Phone: +61 2 9514 2230
Fax: +61 2 9514 2228
Email: Graham.Nicholson@uts.edu.au

Abstract

The basis for the neuroprotectant effect of D-mannitol in reducing the sensory neurological disturbances seen in ciguatera poisoning, is unclear. Pacific ciguatoxin-1 (P-CTX-1), at a concentration 10 nM, caused a statistically significant swelling of rat sensory dorsal root ganglia (DRG) neurons that was reversed by hyperosmolar 50 mM D-mannitol. However, using electron paramagnetic resonance (EPR) spectroscopy, it was found that P-CTX-1 failed to generate hydroxyl free radicals at concentrations of toxin that caused profound effects on neuronal excitability. Whole-cell patch-clamp recordings from DRG neurons revealed that both hyper- and iso-osmolar 50 mM D-mannitol prevented the membrane depolarisation and repetitive firing of action potentials induced by P-CTX-1. In addition, both hyper- and iso-osmolar 50 mM D-mannitol prevented the hyperpolarising shift in steady-state inactivation and the rise in leakage current through tetrodotoxin (TTX)-sensitive Na_v channels, as well as the increased rate of recovery from inactivation of TTX-resistant Na_v channels induced by P-CTX-1. D-Mannitol also reduced, but did not prevent, the inhibition of peak TTX-sensitive and TTX-resistant I_{Na} amplitude by P-CTX-1. Additional experiments using hyper- and iso-osmolar D-sorbitol, hyperosmolar sucrose and the free radical scavenging agents Trolox® and L-ascorbic acid showed that these agents, unlike D-mannitol, failed to prevent the effects of P-CTX-1 on spike electrogenesis and Na_v channel gating. These selective actions of D-mannitol indicate that it does not act purely as an osmotic agent to reduce swelling of nerves, but involves a more complex action dependent on the Na_v channel subtype, possibly to alter or reduce toxin association.

1. Introduction

Ciguatoxins are heat-stable, lipophilic cyclic polyether toxins that originate from the benthic dinoflagellate, *Gambierdiscus* spp. and accumulate in tropical and semi-pelagic reef fish via the marine food chain (Lewis, 2001). The human intoxication syndrome, termed ciguatera, is a form of ichthyosarcotoxism caused by eating fish that have bioaccumulated gambiertoxins, the precursor toxins that are presumably oxidised to ciguatoxins in the liver of fish (Murata et al., 1990). Ciguatera causes significant morbidity, affecting approximately 25,000 people worldwide each year (Lewis, 2001). Of the many congeners of ciguatoxins that have been identified from the Indo-Pacific and Caribbean regions, Pacific ciguatoxin-1 (P-CTX-1) is the most abundant and the most potent congener (Lewis and Jones, 1997). Signs and symptoms of ciguatera poisoning fall into four main categories: gastrointestinal, neurological, cardiovascular and diffuse pain and weakness. The neurological symptoms are, however, the most distressing and include paraesthesiae, dysaesthesiae, pruritis, arthralgia and myalgia. The reversal of thermal sensation, where cold stimuli are felt as painful and/or hot, is considered a pathognomonic symptom (Schnorf et al., 2002).

Ciguatoxins are potent activators of neuronal voltage-gated sodium (Na_v) channels by binding to neurotoxin receptor site 5 on the Na_v channel (Bidard et al., 1984). This causes membrane depolarisation, spontaneous action potentials and an elevation of $[Na^+]_i$, with resulting oedema (Bidard et al., 1984; Allsop et al., 1986; Benoit et al., 1986; Lewis and Endean, 1986; Molgó et al., 1993; Benoit et al., 1996; Mattei et al., 1999a) . These actions result in a stimulation of transmitter release (Bidard et al., 1984; Molgó et al., 1990; Hamblin et al., 1995). Under voltage-clamp conditions, these actions appear to be the result of hyperpolarising shifts in the voltage dependence of activation of TTX-sensitive Na_v channels (Benoit et al., 1986; Hogg et al., 1998; Strachan et al., 1999; Hogg et al., 2002). Furthermore, P-CTX-1 induces a TTX-sensitive leakage current in sensory neurons (Strachan et al., 1999) most likely from the spontaneous opening of a sub-population of Na_v channels (Hogg et al., 1998). P-CTX-1 has also been shown to prolong action potential and afterhyperpolarisation duration and stimulate tonic firing in rat dorsal root ganglion (DRG) neurons as a result of a block of delayed-rectifier and A-type voltage-gated potassium (K_v) channels (Birinyi-Strachan et al., 2004).

Treatment of ciguatera with intravenous infusions of hyperosmotic D-mannitol, an acyclic sugar alcohol (polyol), has gained acceptance as the most effective method of abating the neurological symptoms (Palafox et al., 1988; Pearn et al., 1989). Over 60% of patients have their symptoms reversed by mannitol infusions of 1 g/kg over 30-45 min (Palafox et al., 1988; Pearn et al., 1989). Despite its apparent effectiveness, the mechanism for the neuroprotectant effect of D-mannitol in the treatment of ciguatera is still not fully understood. Most studies indicate that the reduction of cell swelling is the main action of D-mannitol, a well-known osmotic diuretic (Benoit et al., 1996). This

action is supported by the finding that D-mannitol has little effect in reducing the symptoms of ciguatera in mice, due to the marked absence of ciguatoxin-induced axonal oedema in the mouse model (Lewis and Endean, 1983; Lewis et al., 1993). *In vitro* studies have, however, suggested that D-mannitol may exert a more specific role, by interacting with the ciguatoxin molecule itself (Benoit et al., 1996). However, it has also been suggested that D-mannitol may exert its neuroprotectant effect as a scavenger of hydroxyl free radicals (·OH) generated by the ciguatoxin molecule (Pearn et al., 1989; Benoit et al., 1996). D-Mannitol is known to act as a free radical scavenger (Magovern et al., 1984; Desesso et al., 1994). This raises the issue as to whether this action, to prevent alterations in Na_v channel gating, is confined only to mannitol, or is a general property shared by other sugar alcohols (polyols) or osmotic diuretics.

The aims of the present study were, firstly, to determine if P-CTX-1 caused cell swelling in DRG sensory neurons and if D-mannitol was able to reverse this swelling. This effect has been previously identified with amphibian motor nerves but not mammalian sensory neurons (Benoit et al., 1996; Mattei et al., 1997; Mattei et al., 1999b). D-Mannitol was perfused at a concentration of 50 mM as this approximates peak serum levels following a 1 g/kg bolus i.v. dose of mannitol used clinically in the treatment of ciguatera (Cloyd et al., 1986). Secondly, the study aimed to determine if P-CTX-1 was capable of generating free radicals at physiologically relevant concentrations and establish the efficacy of D-mannitol to scavenge or quench these species. This was achieved using the technique of electron paramagnetic resonance (EPR) spectroscopy with spin trapping. The third aim was to determine if hyper or iso-osmolar concentrations of D-mannitol prevented or reversed the actions of P-CTX-1 on Na_v gating and spike electrogenesis in mammalian neurons. The final aim was to determine if other osmotic agents such as D-sorbitol (an isomer of D-mannitol), and sucrose at the same concentration of 50 mM, or known free radical scavengers (Trolox® and L-ascorbic acid) prevented the actions of P-CTX-1 on Na_v channel gating and spike electrogenesis. These final two aims were investigated using whole-cell patch-clamp recording from rat DRG neurons.

2. Materials and Methods

2.1. Isolation and purification of P-CTX-1.

Pacific ciguatoxin-1 was isolated from the viscera of moray eels (*Lycondontis javanicus*) that were collected from a region of Tarawa (1.3°N, 173°E) in the Republic of Kiribati (central Pacific Ocean) where ciguatera is endemic. The isolation and purification techniques required to extract P-CTX-1 have been previously described (Lewis et al., 1991). P-CTX-1 stock (>95% pure) was dissolved in 50% aqueous methanol and stored in glass at –20 °C until when it was diluted with external solution. Control experiments were performed with 50% aqueous methanol at a maximum concentration of 2.2 mg/ml to assess the effects of the vehicle on neuronal excitability, Na_v channel

gating and the generation of free radicals.

2.2. DRG Isolation and Preparation.

DRG neurons, or their afferent fibres, have been previously identified to be sites of ectopic impulse generation leading to the types of sensory paraesthesiae and dysaesthesiae (Wall and Devor, 1983; Rizzo et al., 1996) reported clinically in ciguatera. All cell size, electron paramagnetic resonance and electrophysiological experiments were carried out using acutely dissociated newborn rat DRG neurons isolated as previously described (Nicholson et al., 1994). All procedures were approved by the joint Animal Care and Ethics Committee of the University of Technology, Sydney and the Royal North Shore Hospital.

2.3. Cell Size Experiments.

Glass coverslips, with adherent DRG neurons, were transferred to a perfusion chamber containing a glass graticule with 100 x 100 μm calibration squares on its base. Physiological external solution identical to that used in the voltage-clamp studies (see section 2.6) was used to perfuse the recording chamber. The chamber was mounted on the stage of an inverted reverse-phase polarised microscope (Axiovert 100, Zeiss, Germany) with continuous image projection. A CCD camera was connected to a PC running the AxonImaging Workbench software system (Axon Instruments, Foster City, CA) and continuous stream video used to monitor the neurons and freeze frame digital images acquired for data analysis. Around ten round DRG neurons of similar size and with no neurite processes were chosen on each coverslip and their precise location noted by use of the graticule. Digital images of each cell were taken under control conditions, following a 20-40 min perfusion in 5 or 10 nM P-CTX-1, and following a 20-40 min perfusion in hyperosmolar 50 mM D-mannitol.

2.4. Electron Paramagnetic Resonance Spectroscopy

A Bruker™ EMX X-band EPR spectrometer, equipped with a 100 kHz modulation and a flattened quartz sample cell (Wilmad, NJ, USA), was used for all analyses. EPR spectra were recorded using the manufacturer's acquisition software, WinEPR (Bruker-Franzen Analytic GmbH, Germany). Hydroxyl free radical production was investigated by, EPR spin trapping using the spin trap 5,5-dimethyl-1-pyrroline-*N*-oxide (DMPO), with the magnetic field scanned between 3440 and 3520 G, which is within the organic radical range (Davies, 1997). The DMPO adduct of the hydroxyl free radical was identified by comparison of the line shape, hyperfine coupling constants and *g* value with published reference data (Buettner, 1987). The EPR signal intensity (line height) is directly proportional to the radical concentration, and was used to compare radical concentrations for spectra recorded using identical spectrometer settings (Weil et al., 1994).

Initial experiments were designed to identify free radicals produced by P-CTX-1. The trapping

agent, 5,5-dimethyl-1-pyrroline-*N*-oxide (DMPO) was added to the sample tube as it forms spin adducts (secondary radicals) with hydroxyl radicals (DMPO-OH), which can be easily measured by EPR spectroscopy (Buettner, 1987). Control experiments were carried out in the presence of 10 mM or 55 mM DMPO and the vehicle, 50% aqueous methanol.

In order to determine if the presence of biological tissue was required for the generation of free radicals by P-CTX-1, DRG neurons were incubated with P-CTX-1 and the trapping agent prior to EPR spectroscopy. Dissociated DRG cell density was determined using a haematocytometer and densities of >10 neurons/20 µl of DMEM were used. Up to 960 µl of DMEM culture media, containing dissociated DRG neurons were pre-incubated in 5, 10 or 80 nM P-CTX-1 for up to 2 hours at 37°C (10% CO_2, 90% humidity). The toxin and cell suspension, in addition to 55 mM DMPO was added to the sample cell. In separate experiments, 50 mM D-mannitol was also pre-incubated for 2 hours with a sample containing 55 mM DMPO, 10 nM P-CTX-1 and DRG neurons in DMEM, to test for any inhibition of free radical production by D-mannitol.

2.5. Electrophysiology.

Electrophysiological experiments employed the patch-clamp recording technique in whole-cell configuration to measure current and voltage changes from single DRG neurons. Neurons were bathed in iso-osmotic normal external solution (see section 2.6). Patch pipettes were pulled from borosilicate glass capillary tubing (Corning 7052 Glass, Warner Corp.) and had resistances of 0.8-2 MΩ. Experiments were performed at 22 °C.

Membrane voltage and current were recorded using an Axopatch 200A patch-clamp amplifier (Axon Instruments) and current and voltage pulse protocols were generated using the pClamp software system (Axon Instruments). Signals were filtered using an internal 5 kHz low-pass, 5-pole Bessel filter (–3 dB) and digitised at 15-25 kHz, depending on protocol length. Leakage and capacitive currents were subtracted electronically with *P-P*/4 procedures and series resistance compensation was >80% for all neurons. The voltage-clamp data recorded in this study were rejected if there were large leak currents upon seal formation or currents showed signs of inadequate space clamping. Current-clamp data were rejected if the initial resting membrane potential was more depolarised than –45 mV.

2.6. Recording solutions.

The effects of P-CTX-1 on action and resting potentials were investigated using current-clamp recordings from DRG neurons. The extracellular solution for current-clamp recordings contained (in mM): 120 NaCl, 3 KCl, 10 D-glucose, 1.8 $CaCl_2$, 1.8 $MgCl_2$, 10 N-2-{hydroxyethyl}piperazine-N'-{2-ethanesulfonic acid} (HEPES-acid) and was adjusted to pH 7.4

using 1 M NaOH. The internal patch pipette solution contained (in mM): 110 KCl, 10 NaCl, 5 HEPES-acid and was buffered to pH 7.0 with 1 M KOH. Action potentials (AP) were elicited by 1-2 ms supramaximal currents delivered every 10 s.

Under voltage-clamp conditions, neurons were initially bathed in normal iso-osmotic external solution containing (in mM): 30 NaCl, 5 CsCl, 1.8 $CaCl_2$, 1 $MgCl_2$, 25 D-glucose, 5 HEPES-acid, 70 tetramethylammonium chloride (TMA-Cl), and 20 tetraethylammonium chloride (TEA-Cl) and the pH was adjusted to 7.4 with TEA-hydroxide. A low $[Na^+]_o$ was used to minimise series resistance compensation and avoid saturation of the patch-clamp amplifier. Patch pipettes in voltage-clamp experiments were filled with an internal solution composed of (in mM): 135 CsF, 10 NaCl, and 5 HEPES-acid. The internal solution was buffered with CsOH to pH 7.0.

The osmolality of electrophysiological solutions was monitored with a vapour pressure osmometer (Gonotec Osmomat 030, Berlin, Germany). For both current-clamp and voltage-clamp experiments the osmolarity of the normal internal and external solutions was adjusted with sucrose to 295-305 mOsm/l, except in iso-osmolar 50 mM D-mannitol and iso-osmolar D-sorbitol recordings, where no adjustment was made as the final osmolarity of these solutions ranged between to 295-305 mOsmol/l. In experiments requiring hyperosmolar solutions, either 50 mM D-mannitol, sucrose or D-sorbitol was added to the control external solution, resulting in a final osmolarity of between 345-355 mOsmol/l. Data were recorded from neurons before (control), 5-10 min after perfusion with osmotic agents or free radical scavengers (treatment control), and subsequently following 10 mins with solutions containing osmotic agents, or free radical scavengers, plus P-CTX-1.

The predominant TTX sensitivity of the Na_v channels present in each neuron was determined prior to current-clamp or voltage-clamp recordings using a modified steady-state Na_v channel inactivation voltage-clamp protocol (Rash et al., 2000). This takes advantage of the separation of steady-state inactivation curves for TTX-sensitive and TTX-resistant Na_v channels (Roy and Narahashi, 1992). Once the identity of the major type of sodium current (I_{Na}) was established, the patch-clamp amplifier was switched over to current-clamp mode and changes in the membrane voltage were measured. In those experiments that assessed the actions of P-CTX-1 on TTX-resistant Na_v channels, 200 nM TTX was applied in the external solution to eliminate any residual TTX-sensitive I_{Na}. Only those neurons that exhibited less than 10% TTX-resistant I_{Na}, as determined from the modified steady-state Na_v channel inactivation profile, were used to determine the actions of P-CTX-1 on TTX-sensitive Na_v channels.

2.7. Chemicals.

All chemicals used were analytical grade and, unless otherwise stated, were obtained from Sigma Chemical Co., St. Louis, MO, USA. Tetrodotoxin (Calbiochem, San Diego, CA), supplied as a

citrate buffer, was made up as a 100 μM stock solution with sterile water and stored at –20°C for up to 6 months. Trolox® (6-hydroxy-2,5,7,8 tetramethylchroman-2-carboxylic acid), supplied by Aldrich Chemicals, and L-ascorbic acid (Vitamin C) were dissolved in external solution immediately prior to use, stored in darkened containers and discarded immediately thereafter. DMPO was purified before use by treatment with activated charcoal and made up in Chelex-treated water.

2.8. Data Analysis.

Numerical data are presented as the mean ± S.E. (n, number of observations). The two-dimensional cell area (in pixels^2) was traced using the Axon Imaging software package (Axon Instruments™, CA, USA). Statistical analysis of cell area data was performed using a one-way ANOVA model for correlated samples (VassarStats™, USA). For electrophysiological experiments statistical analysis of pooled results were undertaken based on a one-way ANOVA model for weighted independent samples to determine sources of variability. Post-hoc pairwise treatment comparisons were performed using a Tukey's HSD analysis from the one-way ANOVA model, at the $P < 0.05$ level. Mathematical curve fitting was accomplished using GraphPad Prism version 4.00 for Macintosh (GraphPad Software, San Diego CA, USA). All curve-fitting routines were performed using non-linear regression analysis employing a least squares method.

The voltage-dependence of Na_v channel activation was determined using a depolarising test pulse from -80 to +70 mV for 50 ms, in 5 mV steps. The peak I_{Na} amplitude at each voltage step was measured and used to construct current-voltage (I_{Na}/V) curves.

The fitted curves for the I_{Na}/V relationships were obtained using the following equation:

$$I_{Na} = g_{max}\left(1 - \frac{1}{1 + \exp\left[\left(V - V_{1/2}\right)/s\right]}\right)\left(V - V_{rev}\right) \qquad \text{Equation 1}$$

where I_{Na} is the amplitude of the peak sodium current at a given test potential, V, g_{max} is the maximal Na^+ conductance, $V_{1/2}$ is the voltage at half-maximal activation, s is the slope factor and V_{rev} is the reversal potential.

To determine steady-state Na_v channel inactivation (h_∞) a standard two-pulse protocol with a 0.5-ms interpulse interval was applied. This consisted of a 1-s conditioning prepulse ($V_{prepulse}$), in which the holding potential of -80 mV was stepped to potentials ranging from -130 to 0 mV in 5 mV increments, followed by a 40-ms test pulse (V_{test}) to -10 mV. Pulses were applied every 10 s. Data were either normalised to the maximum peak current in the control or maximum peak current and fitted using the following Boltzmann equation:

$$h_\infty = \frac{A}{1+\exp[(V-V_{1/2})/k]} \qquad \text{Equation 2}$$

where A is the fraction of control maximal peak I_{Na} (value of 1.0 under control conditions), $V_{1/2}$ is the midpoint of inactivation, k is the slope factor and V is the prepulse voltage.

The recovery from sodium channel inactivation was examined by applying a standard two-pulse protocol with a variable interpulse interval (ΔT). A 300-ms conditioning prepulse (V_{cond}) was applied from a holding potential of –80 mV to –10 mV, followed by a 40-ms test pulse (V_{test}), with an interpulse interval ranging between 0.5 ms and 1 s. The unrecovered I_{Na} fraction was used to assess the rate of recovery from inactivation. Rate constant values were derived by fitting the data to the following double exponential decay function:

$$1 - \frac{I_{test}}{I_{cond}} = A\exp(-t/\tau_f) + B\exp(-t/\tau_s) \qquad \text{Equation 3}$$

where A is the fraction of the total current described by a fast time constant (τ_f), and B is the fraction of the total current described by a slow time constant (τ_s).

3. Results

3.1. Cell Size Experiments.

Perfusion of cells with 5 nM P-CTX-1 for 20 to 30 mins did not significantly increase DRG cell area (n = 66, P = 0.08). Nevertheless, perfusion with 10 nM P-CTX-1 significantly increased average cell area by 3.3 ± 1.6% (n = 29, P = 0.02) from 552.2 ± 42.9 to 578.3 ± 45.3 μm^2. This increase, although numerically small, was statistically significant after pairwise analysis, based on a one-way ANOVA model for correlated samples. These experiments were performed using normal voltage-clamp external solution, which contained a low sodium concentration ($[Na^+]_o$ = 30 mM). This allowed correlation of findings with subsequent patch clamp experiments using P-CTX-1 on DRG neurons. Additional experiments were also performed in the external solution for current-clamp experiments containing a physiological sodium concentration ($[Na^+]_o$ =120 mM). These experiments found that no significant differences in the magnitude of neuronal cell swelling induced by P-CTX-1 in either 120 mM (n = 10) or 30 mM $[Na^+]_o$. Importantly the swelling of DRG cell area was significantly reversed by washout in hyperosmolar 50 mM D-mannitol. Following perfusion with 10 nM P-CTX-1, a 20-40 min washout with toxin-free hyperosmolar 50 mM D-mannitol resulted in a 16.2 ± 4.2% (n = 66, P < 0.0001) decrease in cell area from 578.3 ± 45.3 μm^2 to 500.4 ± 39.6 μm^2.

3.2. Electron Paramagnetic Resonance (EPR) Spectroscopy.

Control incubations containing 10 mM DMPO and the vehicle, 50% aqueous methanol, gave rise to EPR spectra with a characteristic signal consisting of four lines in the ratio 1:2:2:1, which has been assigned to the DMPO-OH adduct (Fig. 1Aa) (Buettner, 1987). Subsequent experiments were performed using P-CTX-1 at a high concentration of 500 nM in the presence of DMPO. The resulting spectrum shown in Fig. 1Ab is typical of four experiments using this concentration of P-CTX-1. As can been seen from Fig. 1A, no significant differences in spectral intensity of the DMPO-OH adduct were found between incubations in the absence and presence of 500 nM P-CTX-1.

The production of free radicals by the P-CTX-1 molecule may require the presence of biological tissue. Therefore 80 nM P-CTX-1 was incubated with non-adherent acutely dissociated DRG cells prior to EPR analysis. Control experiments were carried out in the presence of 55 mM DMPO, the vehicle and DMEM culture media containing suspended DRG neurons (Fig. 1Ba). A higher spin trap concentration was chosen for these experiments because the spectra recorded under these conditions were less intense than in the absence of cells, presumably due to the presence of additional targets for any radicals formed. In the presence of both 80 nM P-CTX-1 and DRG neurons, the intensity of the DMPO-OH signal detected by EPR was significantly greater than that detected in the corresponding controls, indicating a increased production of DMPO-OH and hence ·OH radicals (Fig. 1Bb).

As these concentrations of P-CTX-1 are considerably higher than those that modulate Na_v channel gating and spike electrogenesis, we performed additional EPR experiments with 5 and 10 nM P-CTX-1 and DRG neurons. In addition, these experiments also examined the effectiveness of D-mannitol to quench free radical formation. No observable change in spectral intensity were detected in the presence of either 5 nM (n = 2, data not shown) or 10 nM P-CTX-1 (n = 2, Fig. 1C), indicating minimal increased radical formation under these conditions relative to controls. The inclusion of 50 mM hyperosmolar D-mannitol in the incubation mixtures produced only a minor reduction (<5% change) in the intensity of the DMPO-OH adduct signal in the presence of 10 nM P-CTX-1 and DRG neurons (n = 2, data not shown).

3.3. D-Mannitol prevents the membrane depolarisation and repetitive action potential firing induced by P-CTX-1.

To investigate the effects of D-mannitol on P-CTX-1-induced increases in membrane excitability, rat DRG neurons were held under current-clamp conditions and APs were generated from single depolarising pulses. Following perfusion with 10 nM P-CTX-1 alone the most apparent action was an 11.8 ± 1.6 mV (n = 13, P = 0.00017) depolarisation of the resting membrane potential (E_m) (Fig. 2A). In the present study, this rapid membrane depolarisation was blocked by perfusing neurons with external solution containing either hyper- or iso-osmolar 50 mM D-mannitol, together with 10 nM P-CTX-1 (Fig. 2B-C and Table 1). The mean P-CTX-1-induced depolarisation was significantly

reduced to 0.5 ± 1.3 mV (n = 5, P = 0.001) and 1.6 ± 1.2 mV (n = 8, P = 0.0006) by hyper- or iso-osmolar 50 mM D-mannitol, respectively. These actions were not significantly different from control recordings in the absence of P-CTX-1. Importantly, control experiments with hyper- or iso-osmolar 50 mM D-mannitol alone indicated that 50 mM D-mannitol did not alter E_m (Table 1). Previously, Birinyi-Strachan et al. (2004) also showed that 10 nM P-CTX-1 induced stimulus-locked repetitive firing of AP in DRG neurons expressing TTX-sensitive Na_v channels. Moreover, 1 out of every 4 neurons exposed to P-CTX-1 also underwent spontaneous tonic AP firing. In the present study both the stimulus-locked and spontaneous AP firing was inhibited by perfusion with hyper- or iso-osmolar 50 mM D-mannitol in the presence of 10 nM P-CTX-1.

Hyper- or iso-osmotic D-mannitol solutions failed to inhibit the increase in AP and AHP duration induced by 10 nM P-CTX-1. Nevertheless, the duration of TTX-sensitive AP (measured at 50% AP height, AP_{50}), generated in the presence of 50 mM D-mannitol alone was also significantly increased from 1.3 ± 0.1 ms (n = 22) in controls to 2.3 ± 0.4 ms (n = 5, P = 0.0007) and 2.7 ± 0.4 ms (n = 8, P = 0.0001) in hyper- and iso-osmolar 50 mM D-mannitol, respectively (Fig. 2B-C). Therefore D-mannitol most likely reduces the ability of P-CTX-1 to prolong AP duration given that the combined effects of D-mannitol alone and P-CTX-1 alone were less than additive. Table 1 summarises the changes in E_m and alterations in AP and AHP parameters.

Importantly experiments also showed that perfusion with hyper- or iso-osmotic 50 mM D-sorbitol or hyperosmolar 50 mM sucrose in the absence of toxin did not significantly alter resting or AP parameters compared to controls or each other (see Table 1). This is in contrast to D-mannitol. D-Sorbitol and sucrose both failed to prevent the marked depolarisation of E_m and prolongation of AP duration, measured at 0 mV or 50% of maximal spike amplitude following a 10 min perfusion with 10 nM P-CTX-1 (Table 1). These effects were not significantly different from those recorded in the presence of P-CTX-1 alone. Therefore unlike D-mannitol, hyper- or iso-osmolar 50 mM D-sorbitol or hyperosmolar 50 mM sucrose failed to inhibit changes in membrane excitability induced by 10 nM P-CTX-1 in DRG neurons.

3.4. D-Mannitol inhibits the P-CTX-1 induced rise in the leakage current.

A rise in I_{leak} commenced immediately upon perfusion with P-CTX-1 and was concentration dependent, with an average increase of -0.63 ± 0.12 nA (n = 69) following a 10 min perfusion in 5 nM P-CTX-1 (see Fig. 3). However the average I_{leak} induced by 5 nM P-CTX-1 was significantly reduced to –0.26 ± 0.08 nA (n = 13, P = 0.009) and –0.30 ± 0.1 nA (n = 9, P = 0.015) following a 10 min co-perfusion with hyperosmolar or iso-osmolar 50 mM D-mannitol, respectively (Fig 3, Table 2). Importantly, I_{leak} recorded in the presence of hyperosmolar 50 mM D-mannitol and 5 nM P-CTX-1 was not significantly different from controls (n = 13, P = 0.07), however, there was still a small but

significant increase in mean I_{leak} under iso-osmolar conditions (n = 9, P = 0.02). Importantly, there were no significant changes in I_{leak} measured in either hyper or iso-osmolar 50 mM D-mannitol solutions alone when compared to time-matched controls (Fig. 3, Table 2).

3.5. Actions of osmotic agents on the P-CTX-1 induced reduction in peak I_{Na} *amplitude.*

Perfusion with hyperosmolar 50 mM D-mannitol alone for 10 min had no significant effect on peak TTX-sensitive I_{Na}. However hyperosmolar 50 mM D-mannitol alone did significantly reduce TTX-resistant I_{Na} by 16.5 ± 2.6% (n = 9, P <0.05) compared to controls. Neurons were then perfused with a hyperosmolar external solution containing 50 mM D-mannitol and 5 nM P-CTX-1. Hyperosmolar 50 mM D-mannitol failed to significantly inhibit the reduction in peak I_{Na} amplitude in both TTX-sensitive and TTX-resistant Na_v channels, as shown in Figures 4A and C. Peak TTX-sensitive I_{Na} was reduced by 32.5 ± 7.7% (n = 15, P = 0.004) after a 10 min perfusion with 5 nM P-CTX-1 and 50 mM hyperosmotic D-mannitol (Fig. 4A). This decrease was nearly identical to that of TTX-resistant Na_v channels, where a mean reduction of 33.1 ± 8.8% (n = 9, P = 0.005) in peak I_{Na} was observed in the presence of 5 nM P-CTX-1 and hyperosmolar 50 mM D-mannitol (Fig. 4C). This data is summarised in Table 2. Nevertheless, hyperosmolar D-mannitol most likely inhibits the ability of P-CTX-1 to reduce peak TTX-resistant I_{Na} amplitude given that the combined effects of D-mannitol alone and P-CTX-1 alone were less than additive.

Perfusion with iso-osmolar 50 mM D-mannitol alone for 10 min had no significant effect on either peak TTX-sensitive or TTX-resistant I_{Na}. As under hyperosmolar conditions, iso-osmolar 50 mM D-mannitol failed to inhibit the reduction in peak I_{Na} induced by P-CTX-1. Although the reductions in peak I_{Na} were interestingly smaller in iso-osmolar D-mannitol, they were still significantly different to control, as shown by a 23.4 ± 3.9% (n = 10, P = 0.017) and a 29.8 ± 5.2% (n = 4, P = 0.021) reduction in peak I_{Na} recorded from TTX-sensitive and TTX-resistant Na_v channels, respectively (Table 2). Therefore D-mannitol reduces but does not inhibit the ability of P-CTX-1 to reduce peak TTX-sensitive I_{Na} amplitude.

Control experiments also revealed that there were no significant differences between recordings in the presence of D-sorbitol or sucrose alone and controls for either TTX-sensitive or TTX-resistant I_{Na}, with one exception. Hyperosmolar 50 mM sucrose significantly decreased peak TTX-resistant I_{Na} current by 14.5 ± 5.0% when compared to controls (P < 0.05, n = 8, Table 2). Following perfusion with 5 nM P-CTX-1 in the presence of D-sorbitol or sucrose, peak I_{Na} amplitude was significantly reduced. P-CTX-1 caused a 23.6 ± 3.5% (P = 0.02, n = 4), 33.4 ± 4.9% (P = 0.001, n = 4) and 45 ± 4.8% (P < 0.0001, n = 9) reduction in peak TTX-sensitive I_{Na} in the presence of hyper-, iso-osmolar 50 mM D-sorbitol or hyperosmolar 50 mM sucrose, respectively (Table 3). In addition, P-CTX-1 caused a 30.9 ± 9.8% (P = 0.05, n = 4), 39.7 ± 4.2% (P = 0.001, n = 4) and 33.9 ± 7.1% (P < 0.04, n =

6) reduction in peak TTX-resistant I_{Na} in the presence of hyper-, iso-osmolar 50 mM D-sorbitol or hyperosmolar 50 mM sucrose respectively (Table 3). As with hyper- and iso-osmolar D-mannitol, there were also no significant differences in the reduction in peak I_{Na} between recordings in 5 nM P-CTX-1 in the presence of osmotic agents when compared to recordings in 5 nM P-CTX-1 alone for both TTX-sensitive and TTX-resistant I_{Na}. This indicates that sucrose and D-sorbitol failed to prevent the P-CTX-1-induced inhibition of TTX-sensitive and TTX-resistant I_{Na}.

3.6. Actions of osmotic agents on the P-CTX-1-induced shift in the voltage dependence of TTX-sensitive Na_v activation.

P-CTX-1 caused a hyperpolarising shift in the voltage-dependence of TTX-sensitive Na_v channel activation. Figures 5A-D shows families of TTX-sensitive I_{Na} traces generated by a standard I_{Na}/V protocol (see Fig. 5A *inset*). In initial control experiments, hyperosmolar or iso-osmolar 50 mM D-mannitol alone had no significant effect on the voltage dependence of TTX-sensitive Na_v channel activation compared to controls (Table 2). In the presence of 5 nM P-CTX-1, D-mannitol varied in its ability to inhibit the 13 mV hyperpolarising shift in the $V_{1/2}$ in TTX-sensitive Na_v channels. Perfusion with hyperosmolar 50 mM D-mannitol and 5 nM P-CTX-1 for 10 min resulted in a smaller, but still significant, shift of –11 ± 3 mV in the midpoint of activation for TTX-sensitive Na_v channels compared to controls ($n = 6$, $P = 0.03$). This hyperpolarising shift is evident in the altered threshold of I_{Na} activation observed in the current/voltage (I_{Na}/V) curve (Fig. 5E). In addition, a post-hoc analysis found no significant difference in the $V_{1/2}$ between recordings in hyperosmolar 50 mM D-mannitol and 5 nM P-CTX-1 versus recordings in 5 nM P-CTX-1 alone (Table 2).

In contrast, iso-osmolar 50 mM D-mannitol significantly inhibited the P-CTX-1-induced shift in the voltage-dependence of TTX-sensitive Na_v channel activation (Fig. 5C-D). The mean shift in the voltage-midpoint of activation of only –2 ± 3 mV following a 10 min perfusion in iso-osmolar 50 mM D-mannitol and 5 nM P-CTX-1 was not significantly different from controls (Table 2). These results indicate that iso-osmolar, but not hyperosmolar, 50 mM D-mannitol significantly inhibits the P-CTX-1-induced shift in the voltage dependence of TTX-sensitive Na_v channel activation. The reversal potential (V_{rev}) and slope factor (s) were not significantly altered in the presence of either hyper- or iso-osmolar D-mannitol, either alone or in the presence of 5 nM P-CTX-1.

Perfusion with 50 mM hyperosmolar D-sorbitol or sucrose, or 50 mM iso-osmolar D-sorbitol alone did not cause a significant shift in $V_{1/2}$ when compared to controls or each other. In the presence of hyper- and iso-osmolar D-sorbitol, 5 nM P-CTX-1 caused a significant 13 ± 3 mV ($P < 0.05$, $n = 3$) and 11 ± 3 mV ($P < 0.05$, $n = 4$) hyperpolarising shift in the $V_{1/2}$ for TTX-sensitive Na_v channel activation, respectively, not significantly different to the shift in the presence of 5 nM P-CTX-1 alone (Table 3). No significant changes in the slope factor (s) were noted from the D-sorbitol or sucrose I/V

curves. Hence D-sorbitol failed to inhibit the P-CTX-1-induced hyperpolarising shift in $V_{1/2}$. However, hyperosmolar 50 mM sucrose significantly reduced the shift in $V_{1/2}$ by 5 nM P-CTX-1 to only 5 ± 3 mV. This was significantly different from the –13 ± 1 mV ($P = 0.03$, $n = 7$) shift in $V_{1/2}$ in the presence of P-CTX-1 alone and not significantly different from the $V_{1/2}$ recorded in the presence of hyperosmolar 50 mM sucrose alone (Table 3).

3.7. D-Mannitol prevents the P-CTX-1-induced hyperpolarising shift in TTX-sensitive steady-state sodium channel inactivation (h_∞*).*

P-CTX-1 caused a 22 mV hyperpolarising shift in steady-state TTX-sensitive Na_v channel inactivation Figure 6A shows typical TTX-sensitive I_{Na} traces recorded at three different prepulse potentials (–130, –80 and –40 mV) before, and 10 min following, perfusion with 5 nM P-CTX-1 in the presence of hyperosmolar 50 mM D-mannitol. The peak I_{Na} recorded during the test pulse were then either expressed as a fraction of maximum peak control I_{Na} amplitude (Fig. 6B and D), or normalised to the maximum I_{Na} amplitude (Fig. 6C and E). Firstly, Fig. 6B and D highlight the inability of D-mannitol to completely inhibit the P-CTX-1-induced decrease in peak I_{Na} at all prepulse potentials, as seen in Figure 4. At a prepulse potential of –130 mV, the peak I_{Na} amplitude was reduced by 28 ± 8% ($n = 7$) and 29 ± 5% ($n = 9$) in the presence of hyper- and iso-osmolar D-mannitol plus P-CTX-1, respectively. However, perfusion of 5 nM P-CTX-1 in the presence of 50 mM hyperosmolar D-mannitol significantly reduced the hyperpolarising shift in the voltage mid-point of inactivation ($V_{1/2}$) of TTX-sensitive Na_v channel h_∞ to only to +1 ± 3 mV ($n = 7$, $P = 0.0006$). This was not significantly different from controls (Table 2). The shift in the TTX-sensitive Na_v channel h_∞ curve was also prevented by iso-osmolar D-mannitol, reduced to only –2 ± 2 ($n = 9$, $P = 0.0003$), as shown in Figs 6C and E. No significant changes in $V_{1/2}$ were recorded in 50 mM D-mannitol alone. There were also no significant changes in the slope factors (s) of all h_∞ curves recorded in the presence of 50 mM D-mannitol alone.

No significant changes in the voltage mid-point of inactivation ($V_{1/2}$) were recorded in either hyperosmolar 50 mM D-sorbitol or 50 mM sucrose alone, when compared to controls or each other (Table 3). However, perfusion with hyperosmolar D-sorbitol in the presence of 5 nM P-CTX-1 significantly shifted the h_∞ curve 20 ± 4 mV in the hyperpolarising direction ($P = 0.01$, $n = 3$). A similar hyperpolarising shift in $V_{1/2}$ of 15 ± 4 mV ($P = 0.03$, $n = 6$) also occurred after perfusion with hyperosmolar sucrose in the presence of 5 nM P-CTX-1. These hyperpolarising shifts in $V_{1/2}$ were not statistically different to the –22 mV shift induced by P-CTX-1 alone. No significant changes in the slope factor (k) were noted in the hyperosmolar D-sorbitol or sucrose h_∞ curves. These results indicate that both hyperosmolar D-sorbitol and sucrose failed to inhibit the P-CTX-1-induced hyperpolarising shift in TTX-sensitive steady-state Na_v channel inactivation.

3.8. D-Mannitol prevents the action of P-CTX-1 on the rate of recovery from TTX-resistant Na_v channel inactivation.

P-CTX-1 increased the rate of recovery of inactivation in TTX-resistant I_{Na}. In the unrecovered fraction this was seen as a significant increase in coefficient *A* (with a corresponding decrease in coefficient *B*) describing the fast time constant (τ_f) from 0.40 ± 0.04 to 0.64 ± 0.05, and a decrease in τ_f from 9.1 ± 1.2 ms to 4.5 ± 0.9 ms. This indicates an increase in the rate of channel repriming kinetics (Table 2). In the present study, perfusion with hyper or iso-osmolar 50 mM D-mannitol prevented any significant increase in the rate of recovery of TTX-resistant Na_v channel inactivation by 5 nM P-CTX-1. Analysis of the repriming kinetics revealed no significant difference from controls in the time constants or coefficients describing the unrecovered fraction (Fig. 7B and D and Table 2). Also both hyper- and iso-osmolar solutions containing 50 mM D-mannitol in the absence of toxin had no effect on the rate of recovery from inactivation for TTX-resistant I_{Na} (data not shown).

3.9. Ability of hyperosmolar D-mannitol to reverse *the actions of P-CTX-1.*

We also examined the ability of hyperosmolar D-mannitol to reverse the effects of P-CTX-1 on TTX-sensitive and TTX-resistant I_{Na}. To explore this aspect of reversibility, 5 nM P-CTX-1 was added to the external bath solution *prior* to a 25 min washout with hyperosmolar D-mannitol alone (i.e. in toxin-free solution). Three main aspects of Na_v channel gating that were significantly altered by P-CTX-1 were investigated. Firstly, washout in hyperosmolar 50 mM D-mannitol failed to reverse the P-CTX-1-induced reduction in peak I_{Na} amplitude for both TTX-sensitive (n = 7, P = 0.63) and TTX-resistant (n = 5, P = 0.34) Na_v channels (data not shown). Secondly, hyperosmolar 50 mM D-mannitol failed to significantly reverse the large hyperpolarising shift in steady-state inactivation induced by P-CTX-1 in TTX-sensitive Na_v channels, with only 1 out of 7 experiments showed any evidence of reversibility (data not shown). Importantly, this is in contrast to previous experiments where hyperosmolar concentrations of D-mannitol were shown to completely inhibit the hyperpolarising shift in TTX-S steady-state inactivation. In experiments on TTX-resistant Na_v channels, washout with 50 mM hyperosmolar solutions of D-mannitol, also failed to reverse the P-CTX-1-induced increase in the rate of recovery from inactivation (n = 5, data not shown).

3.10. Actions of free radical scavengers on P-CTX-1 modified Na_v channels.

In the present study, EPR spectroscopy identified that at 10 nM P-CTX-1 there was no measurable change in radical adduct signal intensity, although this may be at the limit of resolution of this technique. Therefore it was important to determine whether free radicals contributed to the modulation of Na_v channel gating at a toxin concentration of 10 nM, by assessing the ability of known

free radical scavengers to inhibit or reverse these actions. Trolox® (6-hydroxy-2,5,7,8-tetramethylchroman-2-carboxylic acid), is a water-soluble and cell-permeable analogue of vitamin E. Trolox® has been shown to scavenge free radicals, particularly the hydroxyl radical (Giulivi and Cadenas, 1993) which has been postulated to be generated by ciguatera, with a rate constant, *k,* of 7 x 10^9 dm^3/mol/s (Davies et al., 1988). L-Ascorbic acid (vitamin C), also has a proven experimental record as an anti-oxidant both *in vivo* and *in vitro* (Frei et al., 1989) reacting with hydroxyl radicals with a rate constant, *k*, of 1.1 x 10^{10} dm^3/mol/s (Buxton et al., 1988).

The ability of both Trolox® and L-ascorbic acid to prevent effects of P-CTX-1 on Na_v gating were firstly assessed on I_{Na} amplitude. Cells were perfused with either 100 μM Trolox® or 100 μM L-ascorbic acid for 10-15 minutes prior to addition of 10 nM P-CTX-1. A 10-15 minute perfusion in either 100 μM Trolox® or 100 μM L-ascorbic acid alone did not significantly alter peak TTX-sensitive I_{Na}. However, while Trolox alone did not significantly alter TTX-resistant I_{Na}, L-ascorbic acid alone significantly reduced peak I_{Na} by 14.1 ± 8.4% ($P = 0.04$, $n = 6$) compared to controls. This reduction in peak current was similar to that detected with hyperosmolar D-mannitol or hyperosmolar sucrose alone (see Table 3), which also decreased peak TTX-resistant I_{Na} by 18.5% and 14.5%, respectively. However both Trolox® and L-ascorbic acid failed to significantly reduce the large P-CTX-1-induced inhibition of peak TTX-sensitive and TTX-resistant I_{Na}.

Following perfusion with 10 nM P-CTX-1 in the presence of the free radical scavengers, peak I_{Na} amplitude was significantly reduced. P-CTX-1 caused a 50.5 ± 6.3% ($P < 0.0001$, $n = 5$) and 58.7 ± 3.7% ($P = 0.0001$, $n = 4$) reduction in peak TTX-sensitive I_{Na} in the presence of Trolox® or L-ascorbic acid, respectively (Table 3). In addition, 10 nM P-CTX-1 caused a 67.3 ± 7.4% ($P = 0.0001$, $n = 4$) and 50.6 ± 1.3% ($P = 0.004$, $n = 5$) reduction in peak TTX-resistant I_{Na} in the presence of Trolox® or L-ascorbic acid, respectively (Table 3). As with hyper- and iso-osmolar D-mannitol, there were no significant differences in the reduction in peak I_{Na} between recordings in 10 nM P-CTX-1 in the presence of the free radical scavengers when compared to recordings in 10 nM P-CTX-1 alone for both TTX-sensitive and TTX-resistant I_{Na}. This indicates that Trolox® or L-ascorbic acid failed to prevent the P-CTX-1-induced inhibition of TTX-sensitive and TTX-resistant Na_v channels.

3.11. Trolox® and L-ascorbic acid fail to inhibit the P-CTX-1-induced alterations in the voltage dependence of Na_v channel activation.

Perfusion with 100 μM Trolox® or L-ascorbic acid alone did not cause a significant shift in $V_{1/2}$ when compared to controls. In the presence of 100 μM Trolox® or L-ascorbic acid, 5 nM P-CTX-1 caused a significant 10 ± 2 mV ($P < 0.05$, $n = 5$) and 11 ± 3 mV ($P < 0.05$, $n = 4$) hyperpolarising shift in the $V_{1/2}$ for TTX-sensitive Na_v channel activation, respectively, not significantly different to the –13 ± 1 mV ($n = 7$) shift in the presence of 5 nM P-CTX-1 alone. No significant changes in the slope

factor (*s*) were noted from the Trolox® and L-ascorbic acid *I/V* curves. Therefore these agents failed to prevent the P-CTX-1-induced shift in the voltage dependence of activation.

3.12. Trolox® and L-ascorbic acid fail to inhibit the P-CTX-1-induced alterations in TTX-sensitive Na_v channel steady-state inactivation (h_∞).

Like the osmotic agents tested previously, both Trolox® and L-ascorbic acid failed to inhibit the 22 mV hyperpolarising shift in the TTX-sensitive steady-state Na_v channel inactivation curve induced by 5 nM P-CTX-1. No significant changes in the voltage mid-point of inactivation ($V_{1/2}$) were detected with either 100 μM Trolox® or 100 μM L-ascorbic acid, when compared to controls or each other (Table 3). However, perfusion with 100 μM Trolox® in the presence of 5 nM P-CTX-1 significantly shifted the h_∞ curve 30 ± 6 mV in the hyperpolarising direction (P = 0.001, n = 4). A similar hyperpolarising shift in the $V_{1/2}$ of –23 ± 5 mV (P = 0.01, n = 4) also occurred after TTX-sensitive currents were perfused with hyperosmolar sucrose in the presence of 5 nM P-CTX-1. These hyperpolarising shifts in the $V_{1/2}$ were not statistically different to the –22 ± 4 mV shift induced by P-CTX-1 alone observed previously (Strachan et al., 1999) (Table 3). No significant changes in the slope factor (*k*) were noted in the Trolox® and L-ascorbic acid h_∞ curves.

4. Discussion

The present study shows that P-CTX-1 causes mammalian neuronal cell swelling presumably due to secondary effects following Na^+ loading. Previous studies have shown several strains of ciguatoxin induce swelling of nerves in amphibians (Benoit et al., 1996; Mattei et al., 1997; Mattei et al., 1999a; Mattei et al., 1999b). This appears to be the consequence of continuous Na^+ influx due to persistent activation of Na_v channels at the resting membrane potential and during spontaneous or evoked repetitive firing of action potentials (Benoit et al., 1986; Benoit et al., 1996; Hogg et al., 1998; Strachan et al., 1999). This is accompanied by the influx of water to maintain the osmotic equilibrium resulting in nodal swelling. The sodium loading hypothesis described above is supported by the finding that the sodium channel blocker TTX prevents this swelling (Benoit et al., 1996; Mattei et al., 1997; Mattei et al., 1999a; Mattei et al., 1999b). This swelling has been associated with sensory disturbances, such as alterations to nerve conduction velocity in humans, by increasing the electrical capacitance of the nodal membrane (Allsop et al., 1986; Cameron et al., 1991a; 1991b). This may contribute to the sensory disturbances characteristic of ciguatera poisoning. Additional support is provided in the present study by the lack of a significant alteration in the reversal potential (V_{rev}) for sodium (Fig. 5). Normally, this would be counterbalanced by a compensatory K^+ efflux during repetitive action potentials. However, ciguatoxins have been shown to block K_v channels in DRG neurons (Birinyi-Strachan et al., 2004) and skeletal muscle (Hidalgo et al., 2002).

In comparison to frog myelinated nerve fibres (Mattei et al., 1999a; Mattei et al., 1999b), however, the increase in DRG neuronal cell size due to perfusion with P-CTX-1 was small. The reason for such a large difference in the magnitude of cell swelling most likely lies in the cell preparation used in the present experiments. DRG neurons in physiological solutions are turgid which result in the inability of these cells to swell significantly before detrimental changes occur. Conversely, nodes of Ranvier appear to have a morphology that allows changes in volume more readily, especially in their ability to increase, or even double in size.

Despite the minor effects of P-CTX-1 on DRG neuronal swelling, the changes in cell size, although smaller than in amphibian preparations, still indicate that P-CTX-1 acts to induce a measurable swelling in mammalian sensory neurons that may contribute to some of the effects of the toxin. The present study also shows for the first time that hyperosmolar D-mannitol does reduce swelling following perfusion of DRG sensory neurons with P-CTX-1 and that this may contribute to its action as a neuroprotectant in ciguatera poisoning to reduce paraesthesiae and dysaesthesiae.

Importantly, the present study has also shown that both hyper- and iso-osmolar D-mannitol significantly reduce the majority of the effects of P-CTX-1 on Na_v channel gating and spike electrogenesis in mammalian sensory neurons. Under normal conditions P-CTX-1 induced a concentration-dependent reduction in both TTX-sensitive and TTX-resistant peak I_{Na} amplitude. Perfusion of D-mannitol in hyper- and iso-osmolar conditions failed to fully prevent this action. However, it is important to note that hyperosmolar D-mannitol in the absence of toxin acts to decrease peak I_{Na} amplitude and thus overall there was a significant reduction in the effect of P-CTX-1 (Table 2). Another interesting finding in this study was the ability of iso-osmolar, but not hyperosmolar concentrations of D-mannitol to inhibit the P-CTX-1-induced hyperpolarising shift in the voltage-dependence of TTX-sensitive Na_v channel activation. Overall, however, these actions clearly demonstrate that D-mannitol has a direct action to inhibit increases in neuronal excitability presumably independent of any osmotic actions to reduce nerve cell swelling. Therefore the therapeutic actions of D-mannitol to reduce sensory neurological disturbances are most likely due to a dual action. Firstly, a direct action of D-mannitol to inhibit the rapid modulation of Na_v channel gating leading to membrane depolarisation and tonic or evoked repetitive action potential firing. Secondly, an osmotic action of hyperosmolar D-mannitol to reduce the delayed nodal swelling caused by a continual Na^+ influx resulting from the aforementioned modulation of Na_v channel gating and block of compensatory K^+ efflux via K_v channels (Hidalgo et al., 2002; Birinyi-Strachan et al., 2004).

Interestingly, hyperosmolar D-mannitol solutions also partially inhibited the increase in AP duration due to the perfusion of P-CTX-1. This increase in AP duration is the result of a P-CTX-1-induced block of various K_v channels (Benoit and Legrand, 1994; Birinyi-Strachan et al., 2004) and not a slowing of Na_v channel inactivation (Strachan et al., 1999). These findings therefore

suggest that D-mannitol directly affects the association of P-CTX-1 with certain subtypes of Na_v and possibly K_v, channels present in DRG neurons, in concert with its action to reverse any cell swelling induced by Na^+ loading.

Prolonged washout in toxin-free D-mannitol solutions did not reverse the P-CTX-1-induced reduction in peak I_{Na} the hyperpolarising shift in steady-state inactivation or the increase in the rate of recovery from inactivation. The ability of pre, but not post-application of D-mannitol to inhibit the effect of P-CTX-1 on I_{Na} amplitude, indicates that D-mannitol reduces P-CTX-1 association rates, but has little effect on P-CTX-1 dissociation rates in mammalian sensory neurons. Such an action supports the findings that mannitol is most effective in treating ciguatera early in the course of the disease (Schnorf et al., 2002).

To determine if the above actions were specific for D-mannitol, further experiments investigated the ability of the structurally related acyclic polyol, D-sorbitol, and the unrelated cyclic sugar, sucrose, to inhibit these P-CTX-1-induced changes in neuronal excitability. Under voltage- and current-clamp conditions, D-sorbitol and sucrose failed to prevent P-CTX-1 induced increases in neuronal excitability further emphasising the unique action of D-mannitol to inhibit P-CTX-1-induced alterations in spike electrogenesis.

Previous studies have postulated that ciguatoxins may generate hydroxyl free radicals given the highly oxygenated nature of the cyclic polyether structure (Pearn et al., 1989; Benoit et al., 1996). In support of this postulate, D-mannitol is a known scavenger of hydroxyl radicals with a rate constant, k, of 1.7 x 10^9 dm^3/mol/s (Buxton et al., 1988). Therefore the neuroprotectant action of D-mannitol may be due to this action. This is the first study to show that only high concentrations of P-CTX-1 produce free radicals and only in the presence of biological tissue. The mechanism for this generation of hydroxyl radicals is presently unknown and it cannot be excluded that high concentrations of P-CTX-1 do not cause cell apoptosis leading to production of free radicals. Importantly, P-CTX-1 at very high concentrations (500 nM) did not generate free radicals in the absence of biological tissue. In addition, it appears that 5-10 nM P-CTX-1, concentrations that produce profound alterations in spike electrogenesis and Na_v channel gating, fail to produce measurable amounts of hydroxyl free radicals. Thus while P-CTX-1 may generate hydroxyl free radicals, significant levels only occur at doses much higher than those that alter neuronal excitability.

One possible limitation of the EPR experiments could be that generation of free radicals at low P-CTX-1 concentrations, sufficient to alter neuronal excitability, are below the limit of detection using EPR spectroscopy. To investigate this possibility, patch clamp experiments were carried out to determine if known and highly efficacious free radical scavengers could prevent the actions of P-CTX-1. Accordingly voltage-clamp experiments investigated the ability of Trolox® with a rate constant for reaction with hydroxyl radicals, k, of 7 x 10^9 dm^3/mol/s (Davies et al., 1988) and L-

ascorbic acid with a k value of 1.1 x 10^{10} dm^3/mol/s (Buxton et al., 1988), to inhibit these P-CTX-1-induced changes in neuronal excitability. Unlike the actions of D-mannitol, both of these free radical scavengers failed to inhibit any of the P-CTX-1-induced alterations in Na_v channel gating. These results again suggest a different mechanism of action of D-mannitol in inhibiting P-CTX-1 effects on sodium channels, compared to the other osmotic and radical scavenging agents. Finally, it is salient to note that sucrose, which has a rate constant, k, of 2.3 x 10^9 dm^3/mol/s for reaction with hydroxyl radicals, is a more efficacious scavenger of free radicals than D-mannitol, with a k value of 1.7 x 10^9 dm^3/mol/s. Indeed, even D-sorbitol is comparable to D-mannitol with a rate constant of 1.5 x 10^9 dm^3/mol/s. Therefore since hyperosmolar sucrose failed to prevent any of the alterations in channel gating or spike electrogenesis it is highly unlikely that the neuroprotectant effect of D-mannitol in mammalian DRG neurons is due solely to a osmotic reduction of neuronal swelling or the scavenging of hydroxyl free radicals. In addition, D-mannitol is unlikely to directly detoxify the polyether toxin, since spontaneous nerve activity reappears rapidly upon washout of D-mannitol in many preparations (Mattei et al., 1999b), albeit not in DRG neurons. These data and previous studies indicate that additional actions of mannitol to inhibit toxin association (k_{on}) with the Na_v channel may play an important role. Future experiments could address this using radioligand binding studies.

The findings of the present study suggest that the neuroprotectant action of D-mannitol on DRG Na_v channels involves a direct effect on toxin association to receptor site 5, but not on its displacement from the Na_v channel. Thus at iso-osmolar concentrations, D-mannitol prevents but does not reverse the actions of P-CTX-1. This is in accordance with the inability of D-mannitol to reverse ciguatoxin-induced changes in DRG Na_v channel gating after sustained washout. Presently, other evidence to suggest that prior incubation with iso-osmotic D-mannitol prevents subsequent binding of site 5 neurotoxins such as ciguatoxin, or other site 5 neurotoxins, is lacking. This action on Na_v channels expressed in DRG neurons differs from effects in other preparations where post-application of hyperosmolar concentrations of D-mannitol (Benoit et al., 1996; Mattei et al., 1999b), hyperosmolar sucrose or TMA (Benoit et al., 1996) reversed the effects of ciguatoxin. However, given that hyperosmolar solutions not containing mannitol are also effective indicates that these effects may arise through the reduction in nodal swelling, prominent in amphibian preparations.

Despite clear prevention of the effects of P-CTX-1 on the gating of DRG Na_v channels, D-mannitol appears to have limited effect on the signs of toxicity or survival of mice (Lewis et al., 1993). In addition, mannitol fails to prevent the actions of P-CTX-1 on human atrial trabeculae (Lewis et al., 1992) but, to varying degrees, it does inhibit actions on motor nerve fibres (Lewis et al., 1993). Given that humans experience, in many cases, a rapid relief of the sensory neurological symptoms of acute ciguatera, it would appear that the neuroprotectant effects of mannitol treatment appears to be mainly confined to Na_v channels mediating sensory and, in some cases, motor function and not those

associated with autonomic or cardiac function. D-Mannitol also appears not to reverse or prevent toxic effects of central origin in mice or cats (Lewis et al., 1993) although this may due to the rapid effects in theses species or subtle differences in sodium channel subtypes between species. Thus ciguatoxins appear to target one or several of the TTX-sensitive DRG Na_v subtypes including $Na_v1.1$, $Na_v1.6$ or $Na_v1.7$ that have been shown to be highly expressed in DRG neurons (for a review of Na_v subtypes see (Catterall, 2000). Given the limited actions of P-CTX-1 on DRG neurons expressing TTX-resistant Na_v channels, it would appear that the $Na_v1.8$ and $Na_v1.9$ channel subtypes are not involved to any appreciable extent. From previous work, ciguatoxins appear to modulate $Na_v1.7$ expressed in motor nerves (Benoit et al., 1996) and $Na_v1.4$ expressed in skeletal muscle (Hidalgo et al., 2002; Bottein Dechraoui and Ramsdell, 2003). However there appear to be conflicting reports of actions on the cardiac Na_v channels. In isolated cardiac muscle preparations, ciguatoxins only have a direct action at high concentrations, with an indirect action mediated via nerve-evoked noradrenaline release predominating at lower concentrations (Lewis and Endean, 1986; Seino et al., 1988; Lewis et al., 1992; Sauviat et al., 2002). This is borne out clinically with only severe cases presenting with cardiac problems. However, this is in contrast to potent actions of P-CTX-3C in radioligand binding experiments using HEK293 cells expressing cardiac $Na_v1.5$ (hH1) channels (Bottein Dechraoui and Ramsdell, 2003). Presently it is unclear which Na_v channels ciguatoxins target in the CNS ($Na_v1.1$, 1.2, 1.3 or 1.6), but they do target $Na_v1.2$ in rat brain synaptosomes (Bidard et al., 1984; Bottein Dechraoui and Ramsdell, 2003), the predominant subtype in this preparation (Gordon et al., 1987).

In conclusion, the role of mannitol in reversing the symptoms of ciguatera is not limited to an osmotic reduction of peripheral nodal swelling, but rather involves a more complex process possibly involving an inhibition of toxin association with Na_v channels. Future experiments should address this issue using radioligand binding techniques. The differences in the effects of ciguatoxins between DRG neurons and other mammalian or amphibian preparations may also relate to the unique Na_v channel subtypes present in these sensory cell bodies in this species. Therefore future studies are required to determine which Na_v channel subtypes are the target for ciguatoxins.

Acknowledgements

This work was supported by an Australian Postgraduate Award to L.B-S., a UTS internal research grant to G.M.N. and an Australian Research Council fellowship to M.J.D.

References

Allsop, J.L., Martini, L., Lebris, H., Pollard, J., Walsh, J., Hodgkinson, S., 1986. Les manifestations neurologiques de la ciguatera. Rev. Neurol. (Paris) 142, 590-597.

Benoit, E., Juzans, P., Legrand, A.-M., Molgó, J., 1996. Nodal swelling produced by ciguatoxin-

induced selective activation of sodium channels in myelinated nerve fibers. Neuroscience 71, 1121-1131.

Benoit, E., Legrand, A.-M., 1994. Gambiertoxin-induced modifications of the membrane potential of myelinated nerve fibres. Mem. Queensland Mus. 34, 461-464.

Benoit, E., Legrand, A.-M., Dubois, J.M., 1986. Effects of ciguatoxin on current and voltage clamped frog myelinated nerve fibre. Toxicon 24, 357-364.

Bidard, J.N., Vijverberg, H.P., Frelin, C., Chungue, E., Legrand, A.-M., Bagnis, R., Lazdunski, M., 1984. Ciguatoxin is a novel type of Na^+ channel toxin. J. Biol. Chem. 259, 8353-8357.

Birinyi-Strachan, L.C., Gunning, S.J., Lewis, R.J., Nicholson, G.M., 2004. Block of voltage-gated potassium channels by Pacific ciguatoxin-1 contributes to increased neuronal excitability in rat sensory neurons. Toxicol. Appl. Pharmacol. in press.

Bottein Dechraoui, M.Y., Ramsdell, J.S., 2003. Type B brevetoxins show tissue selectivity for voltage-gated sodium channels: comparison of brain, skeletal muscle and cardiac sodium channels. Toxicon 41, 919-927.

Buettner, G.R., 1987. Spin trapping: ESR parameters of spin adducts. Free Radic. Biol. Med. 3, 259-303.

Buxton, G.V., Greenstock, C.L., Helman, W.P., Ross, A.B., 1988. Critical review of rate constants for reactions of hydrated electrons, hydrogen atoms and hydroxyl radicals ($\bullet OH/\bullet O^-$) in aqueous solution. J. Phys. Chem. Ref. Data 17, 513-886.

Cameron, J., Flowers, A.E., Capra, M.F., 1991a. Effects of ciguatoxin on nerve excitability in rats (Part I). J. Neurol. Sci. 101, 87-92.

Cameron, J., Flowers, A.E., Capra, M.F., 1991b. Electrophysiological studies on ciguatera poisoning in man (Part II). J. Neurol. Sci. 101, 93-97.

Catterall, W.A., 2000. From ionic currents to molecular mechanisms: the structure and function of voltage-gated sodium channels. Neuron 26, 13-25.

Cloyd, J.C., Snyder, B.D., Cleeremans, B., Bundlie, S.R., Blomquist, C.H., Lakatua, D.J., 1986. Mannitol pharmacokinetics and serum osmolality in dogs and humans. J. Pharmacol. Exp. Ther. 236, 301-306.

Davies, M.J., 1997. EPR Spectroscopy: electrons on the loose. Life Sciences 7, 30-35.

Davies, M.J., Forni, L.G., Willson, R.L., 1988. Vitamin E analogue Trolox C. E.s.r. and pulse-radiolysis studies of free-radical reactions. Biochem. J. 255, 513-522.

Desesso, J.M., Scialli, A.R., Goeringer, G.C., 1994. D-mannitol, a specific hydroxyl free radical scavenger, reduces the developmental toxicity of hydroxyurea in rabbits. Teratology 49, 248-259.

Frei, B., England, L., Ames, B.N., 1989. Ascorbate is an outstanding antioxidant in human blood plasma. Proc. Natl. Acad. Sci. U S A 86, 6377-6381.

Giulivi, C., Cadenas, E., 1993. Inhibition of protein radical reactions of ferrylmyoglobin by the water-soluble analog of vitamin E, Trolox C. Arch. Biochem. Biophys. 303, 152-158.

Gordon, D., Merrick, D., Auld, V., Dunn, R., Goldin, A.L., Davidson, N., Catterall, W.A., 1987. Tissue-specific expression of the R_I and R_{II} sodium channel subtypes. Proc. Natl. Acad. Sci. USA 84, 8682-8686.

Hamblin, P.A., McLachlan, E.M., Lewis, R.J., 1995. Sub-nanomolar concentrations of ciguatoxin-1 excite preganglionic terminals in guinea pig sympathetic ganglia. Naunyn-Schmiedeberg's Arch. Pharmacol. 352, 236-246.

Hidalgo, J., Liberona, J.L., Molgo, J., Jaimovich, E., 2002. Pacific ciguatoxin-1b effect over Na+ and K+ currents, inositol 1,4,5-triphosphate content and intracellular Ca2+ signals in cultured rat myotubes. Br J Pharmacol 137, 1055-1062.

Hogg, R.C., Lewis, R.J., Adams, D.J., 1998. Ciguatoxin (CTX-1) modulates single tetrodotoxin-sensitive sodium channels in rat parasympathetic neurones. Neurosci. Lett. 252, 103-106.

Hogg, R.C., Lewis, R.J., Adams, D.J., 2002. Ciguatoxin-induced oscillations in membrane potential and action potential firing in rat parasympathetic neurons. Eur. J. Neurosci. 16, 242-248.

Lewis, R.J., 2001. The changing face of ciguatera. Toxicon 39, 97-106.

Lewis, R.J., Endean, R., 1983. Occurrence of a ciguatoxin-like substance in the Spanish mackerel (*Scomberomorus commersoni*). Toxicon 21, 19-24.

Lewis, R.J., Endean, R., 1986. Direct and indirect effects of ciguatoxin on guinea-pig atria and papillary muscles. Naunyn-Schmiedeberg's Arch. Pharmacol. 334, 313-322.

Lewis, R.J., Hoy, A.W., McGiffin, D.C., 1992. Action of ciguatoxin on human atrial trabeculae. Toxicon 30, 907-914.

Lewis, R.J., Hoy, A.W., Sellin, M., 1993. Ciguatera and mannitol: *in vivo* and *in vitro* assessment in mice. Toxicon 31, 1039-1050.

Lewis, R.J., Jones, A., 1997. Characterization of ciguatoxins and ciguatoxin congeners present in ciguateric fish by gradient reverse-phase high-performance liquid chromatography/mass spectrometry. Toxicon 35, 159-168.

Lewis, R.J., Sellin, M., Poli, M.A., Norton, R.S., MacLeod, J.K., Sheil, M.M., 1991. Purification and characterization of ciguatoxins from moray eel (*Lycodontis javanicus*, Muraenidae). Toxicon 29, 1115-1127.

Magovern, G.J., Jr., Bolling, S.F., Casale, A.S., Bulkley, B.H., Gardner, T.J., 1984. The mechanism of mannitol in reducing ischemic injury: hyperosmolarity or hydroxyl scavenger? Circulation 70, I91-95.

Mattei, C., Benoit, E., Juzans, P., Legrand, A.-M., Molgó, J., 1997. Gambiertoxin (CTX-4B), purified from wild *Gambierdiscus toxicus* dinoflagellates, induces Na^+-dependent swelling of single frog

myelinated axons and motor nerve terminals *in situ*. Neurosci. Lett. 234, 75-78.

Mattei, C., Dechraoui, M.Y., Molgó, J., Meunier, F.A., Legrand, A.-M., Benoit, E., 1999a. Neurotoxins targetting receptor site 5 of voltage-dependent sodium channels increase the nodal volume of myelinated axons. J. Neurosci. Res. 55, 666-673.

Mattei, C., Molgó, J., Marquais, M., Vernoux, J., Benoit, E., 1999b. Hyperosmolar D-mannitol reverses the increased membrane excitability and the nodal swelling caused by Caribbean ciguatoxin-1 in single frog myelinated axons. Brain Res. 847, 50-58.

Molgó, J., Comella, J.X., Legrand, A.-M., 1990. Ciguatoxin enhances quantal transmitter release from frog motor nerve terminals. Brit. J. Pharmacol. 99, 695-700.

Molgó, J., Shimahara, T., Legrand, A.-M., 1993. Ciguatoxin, extracted from poisonous moray eels, causes sodium-dependent calcium mobilization in NG108-15 neuroblastoma x glioma hybrid cells. Neurosci. Lett. 158, 147-150.

Murata, M., Legrand, A.-M., Ishibashi, Y., Yasumoto, T., 1990. Structures and configurations of ciguatoxin from the moray eel *Gymnothorax javanicus* and its likely precursor from the dinoflagellate *Gambierdiscus toxicus*. J. Am. Chem. Soc. 112, 4380-4386.

Nicholson, G.M., Willow, M., Howden, M.E.H., Narahashi, T., 1994. Modification of sodium channel gating and kinetics by versutoxin from the Australian funnel-web spider *Hadronyche versuta*. Pflügers Archiv. (Eur. J. Physiol.) 428, 400-409.

Palafox, N.A., Jain, L.G., Pinano, A.Z., Gulick, T.M., Williams, R.K., Schatz, I.J., 1988. Successful treatment of ciguatera fish poisoning with intravenous mannitol. JAMA 259, 2740-2742.

Pearn, J.H., Lewis, R.J., Ruff, T., Tait, M., Quinn, J., Murtha, W., King, G., Mallett, A., Gillespie, N.C., 1989. Ciguatera and mannitol: experience with a new treatment regimen. Med. J. Aust. 151, 77-80.

Rash, L.D., Birinyi-Strachan, L.C., Nicholson, G.M., Hodgson, W.C., 2000. Neurotoxic activity of venom from the Australian eastern mouse spider (*Missulena bradleyi*) involves modulation of sodium channel gating. Brit. J. Pharmacol. 130, 1817-1824.

Rizzo, M.A., Kocsis, J.D., Waxman, S.G., 1996. Mechanisms of paresthesiae, dysesthesiae, and hyperesthesiae: role of Na^+ channel heterogeneity. Eur. Neurol. 36, 3-12.

Roy, M.L., Narahashi, T., 1992. Differential properties of tetrodotoxin-sensitive and tetrodotoxin-resistant sodium channels in rat dorsal root ganglion neurons. J. Neurosci. 12, 2104–2111.

Sauviat, M.P., Marquais, M., Vernoux, J.P., 2002. Muscarinic effects of the Caribbean ciguatoxin C-CTX-1 on frog atrial heart muscle. Toxicon 40, 1155-1163.

Schnorf, H., Taurarii, M., Cundy, T., 2002. Ciguatera fish poisoning: a double-blind randomized trial of mannitol therapy. Neurology 58, 873-880.

Seino, A., Kobayashi, M., Momose, K., Yasumoto, T., Ohizumi, Y., 1988. The mode of inotropic

action of ciguatoxin on guinea-pig cardiac muscle. Br J Pharmacol 95, 876-882.

Strachan, L.C., Lewis, R.J., Nicholson, G.M., 1999. Differential actions of Pacific ciguatoxin-1 on sodium channel subtypes in mammalian sensory neurons. J. Pharmacol. Exp. Ther. 288, 379-388.

Wall, P.D., Devor, M., 1983. Sensory afferent impulses originate from dorsal root ganglia as well as from the periphery in normal and nerve injured rats. Pain 17, 321-339.

Weil, J., Bolton, J., Wertz, J., 1994. Electron Paramagnetic Resonance: Elementary Theory and Practical Applications. John Wiley and Sons, New York, USA.

Figure Legends

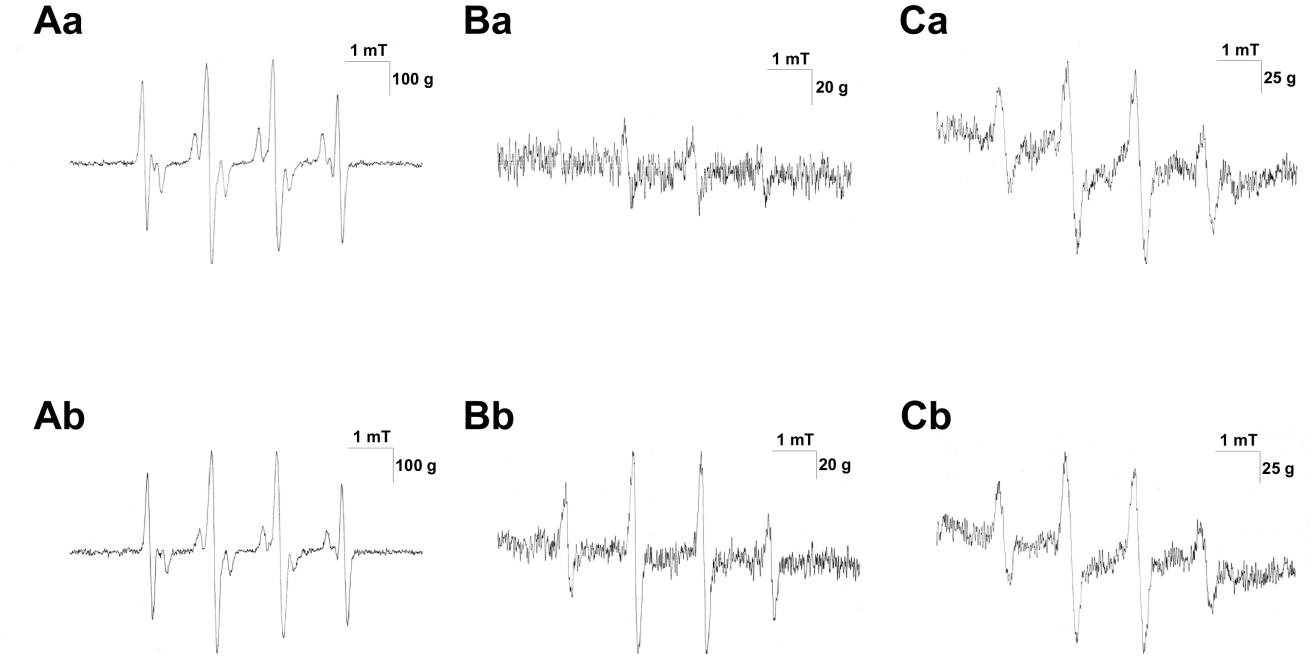

Fig. 1. Hydroxyl free radical formation by P-CTX-1. (Aa) Control spectrum recorded in the presence of 10 mM DMPO trapping agent. (Ab) No increased generation of hydroxyl free radicals, as evidenced by the intensity of the signal from the DMPO-OH adduct, was observed following the addition of 500 nM P-CTX-1. (B) The presence of cellular material was required for ·OH formation by P-CTX-1. (Ba) Control spectra recorded in the presence of 55 mM DMPO and dissociated DRG neurons (>500 cells/ml) in DMEM culture medium. (Bb) Typical increase in spectral intensity amplitude in the presence of 80 nM P-CTX-1, recorded in the presence of DRG neurons and DMPO. (C) Lack of generation of free radicals at concentrations of P-CTX-1 that modulate Na_v channel gating and spike electrogenesis. (Ca) Control spectra were recorded in the presence of 40 mM DMPO trapping agent and DRG neurons. (Cb) No significant generation of radical species occurred in the presence of 10 nM P-CTX-1, recorded in the presence of DRG neurons and DMPO.

Fig 2 AP + mann.pzf:Fig 2 AP + mann - Sun Nov 21 23:43:42 2004

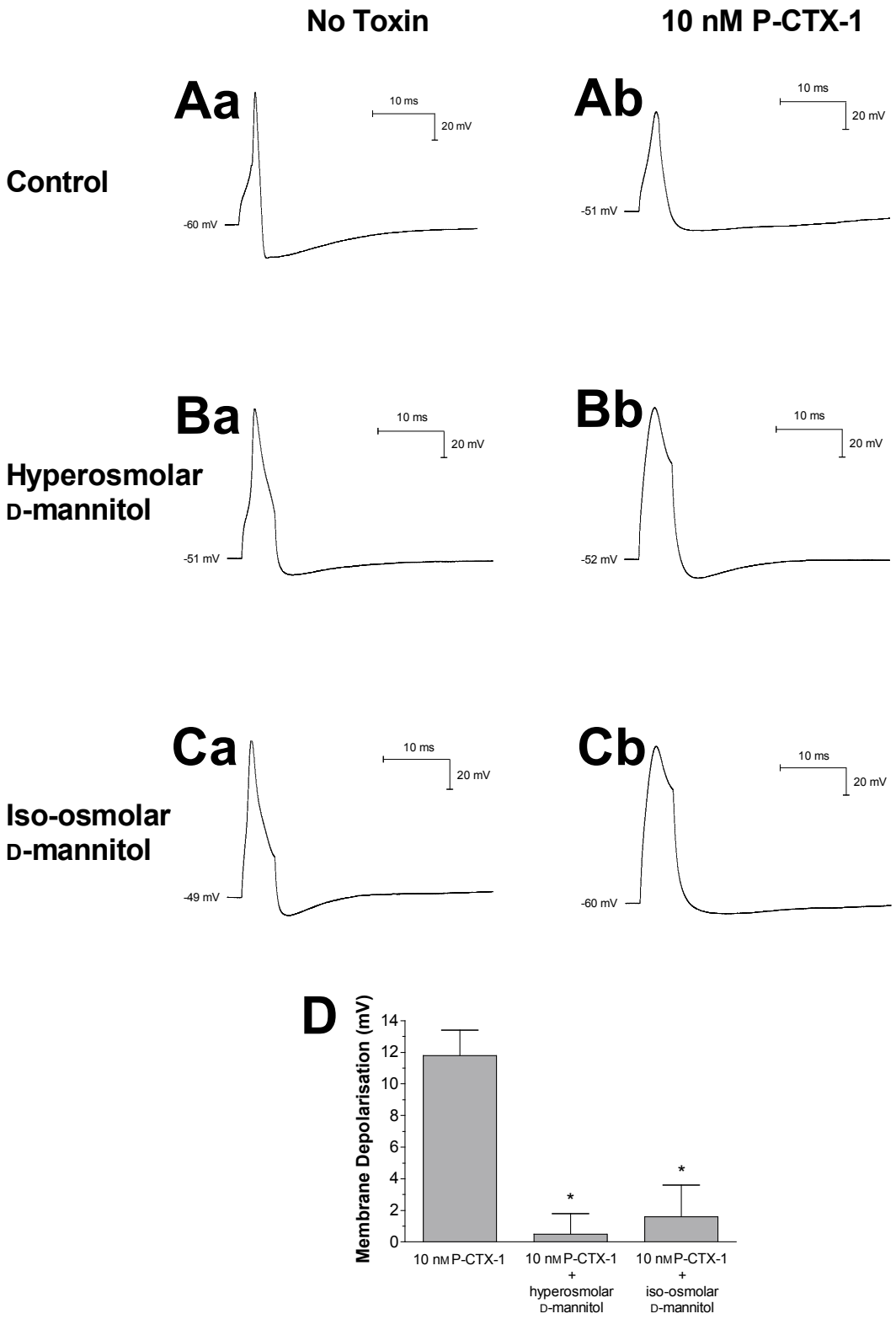

Fig. 2. The effect of D-mannitol on P-CTX-1-modified action potentials (AP) in DRG neurons expressing TTX-sensitive Na_v channels. (A) Superimposed APs generated by supramaximal current

pulses prior to (a), and following (b), perfusion with 10 nM P-CTX-1. Note the membrane depolarisation in the presence of P-CTX-1. (B-C) Typical recordings of the effect of hyperosmolar (B) and iso-osmolar (C) 50 mM mannitol in the presence (b), or absence (a), of 10 nM P-CTX-1.

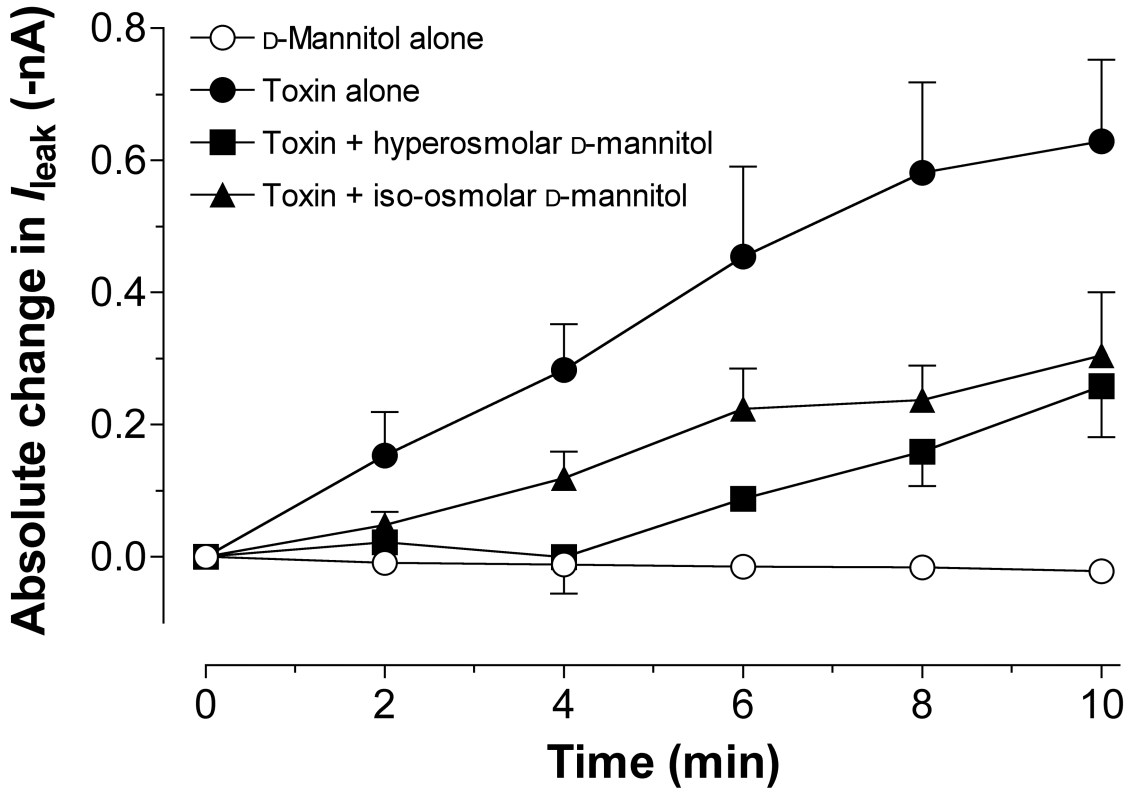

Fig. 3. Action of D-mannitol on the P-CTX-1-induced rise in leakage current (I_{leak}) through TTX-sensitive Na_v channels. Absolute changes in I_{leak} (–nA) were recorded in either (■) hyperosmolar (n = 13) or (▲) iso-osmolar (n = 9) 50 mM D-mannitol solutions. Data were initially recorded during a 10 min perfusion in D-mannitol alone (○). Cells were then perfused for a further 10 mins with 5 nM P-CTX-1 in the presence of either hyper- or iso-osmolar 50 mM D-mannitol. The mean rise in I_{leak} after perfusion with 5 nM P-CTX-1 alone (●) is shown for comparison.

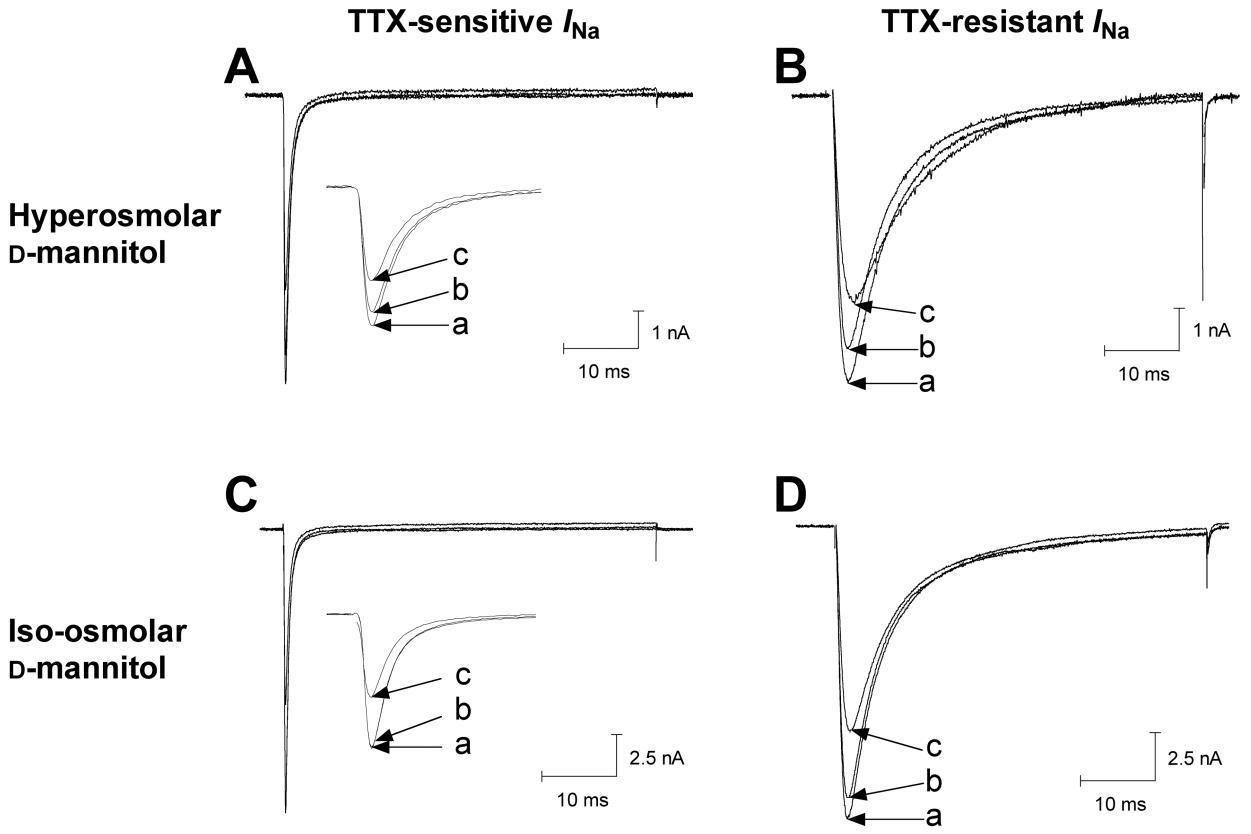

Fig. 4. Actions of D-mannitol on the P-CTX-1-induced inhibition of peak I_{Na}. Depolarising test pulses, from a holding potential of –80 mV to –10 mV for 50 ms every 10 s, were employed to generate TTX-sensitive (A,C) and TTX-resistant (B,D) I_{Na}. Panels show the effects of hyperosmolar (A-B) or iso-osmolar (C-D) 50 mM D-mannitol. Each panel shows superimposed I_{Na} recorded under control conditions (trace *a*), 10 min after perfusion with D-mannitol (trace *b*), and a further 10 min following perfusion with 5 nM P-CTX-1 plus 50 mM D-mannitol (trace *c*). Insets in panels A and C show magnified peak TTX-sensitive I_{Na}.

Fig 4 IV.pzf:Layout 2 - Wed May 26 17:06:39 2004

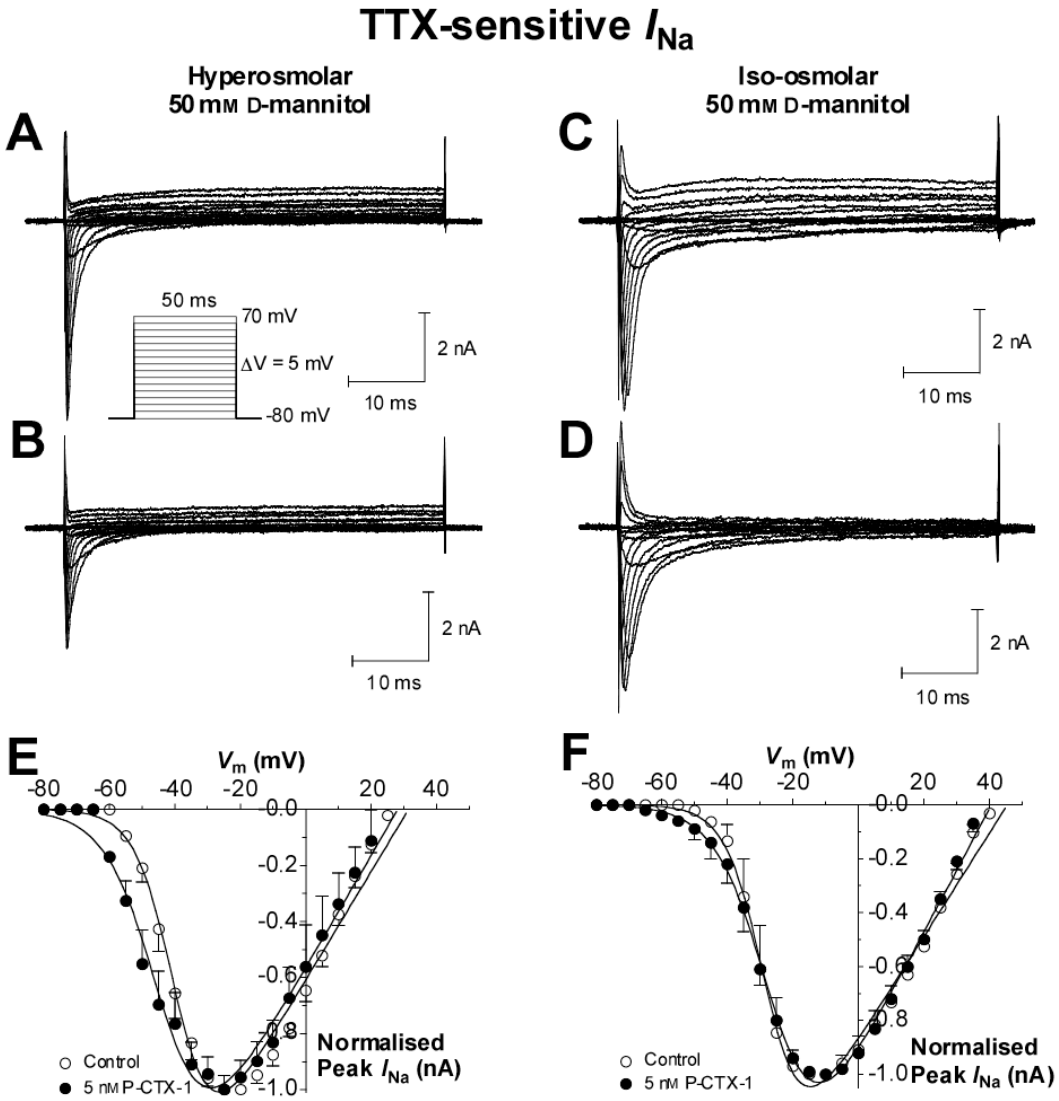

Fig. 5. Actions of D-mannitol on P-CTX-1-induced alterations in the voltage dependence of TTX-sensitive Na_v activation. (A-D) Families of TTX-sensitive I_{Na} were elicited (see inset) before (A, C), and following, a 10 min perfusion with 5 nM P-CTX-1 plus hyperosmolar (B), or iso-osmolar (D), 50 mM D-mannitol. (E-F) Peak current/voltage (I_{Na}/V) relationships are graphed in the absence (○) and presence (●) of 5 nM P-CTX-1 plus hyperosmolar (E) or iso-osmolar (F) 50 mM D-mannitol. For clarity, only I_{Na} recorded in 10 mV steps are presented. Data were normalised to peak inward I_{Na} and then fitted with Equation 1, $n \geq 4$ experiments.

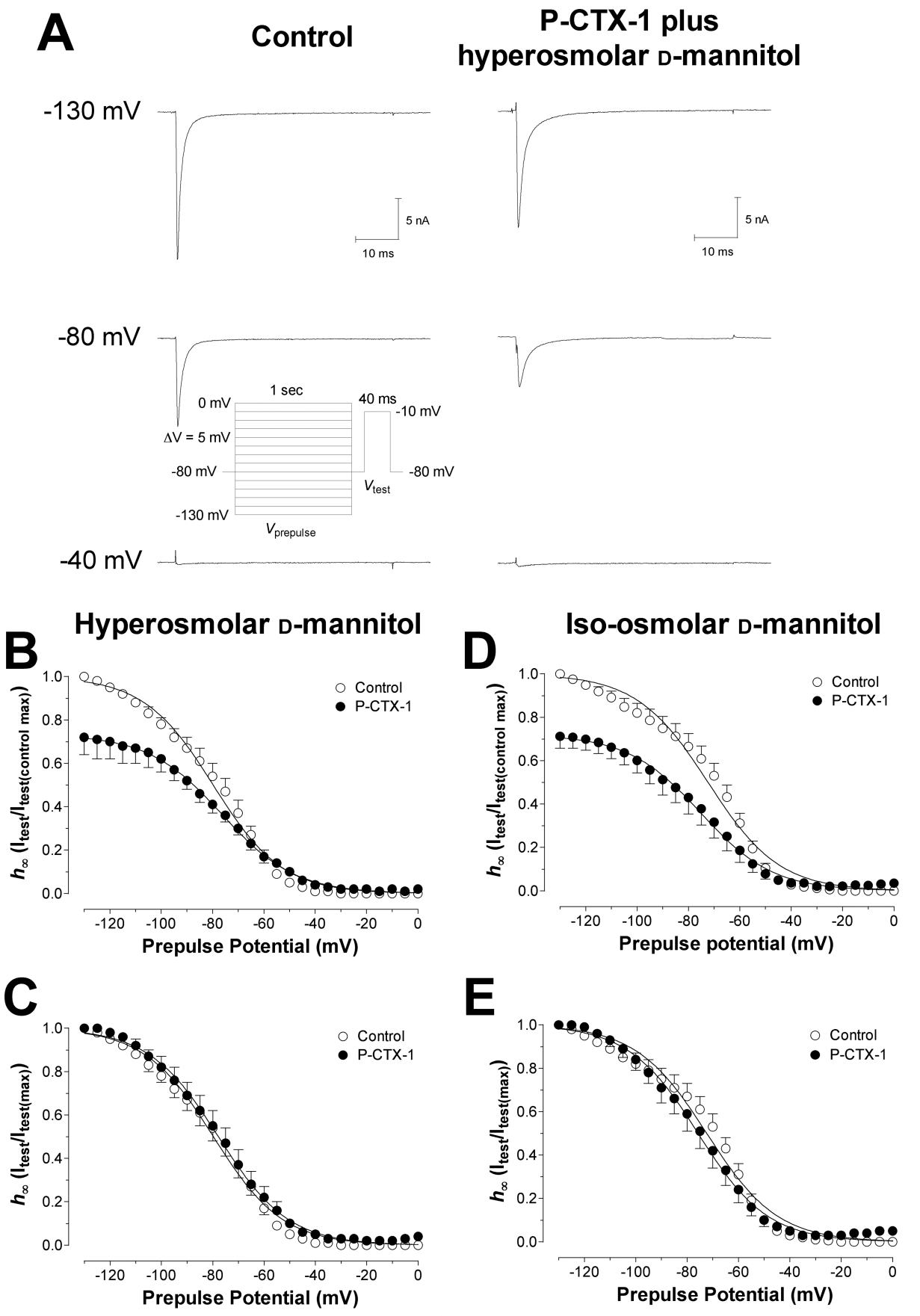

Fig. 6. Effects of D-mannitol on P-CTX-1-induced alterations in steady-state TTX-sensitive Na_v channel inactivation (h_∞). Steady-state inactivation was determined using a two-pulse protocol (see *inset* in A). (A) Typical TTX-sensitive I_{Na} traces obtained following a 40-ms test pulse (V_{test}) to –10

mV subsequent to prepulses of –130, –80 and –40 mV. Current traces were recorded before (left hand traces), and following a 10 min perfusion with 5 nM P-CTX-1 in the presence of hyperosmolar 50 mM D-mannitol (right hand traces). (B-E) Peak I_{Na} recorded during the test pulse were expressed as a fraction of maximum control I_{Na} (B, D) or normalised to peak I_{Na} amplitude (C, E), and plotted against prepulse potential. The amount of I_{Na} that is available for activation under control conditions (○), and during perfusion with 5 nM P-CTX-1 plus 50 mM D-mannitol (●), is shown under hyperosmolar (C-D, $n \geq 9$) and iso-osmolar (E-F, $n \geq 7$) conditions. The h_∞/V curves were fitted to equation 2.

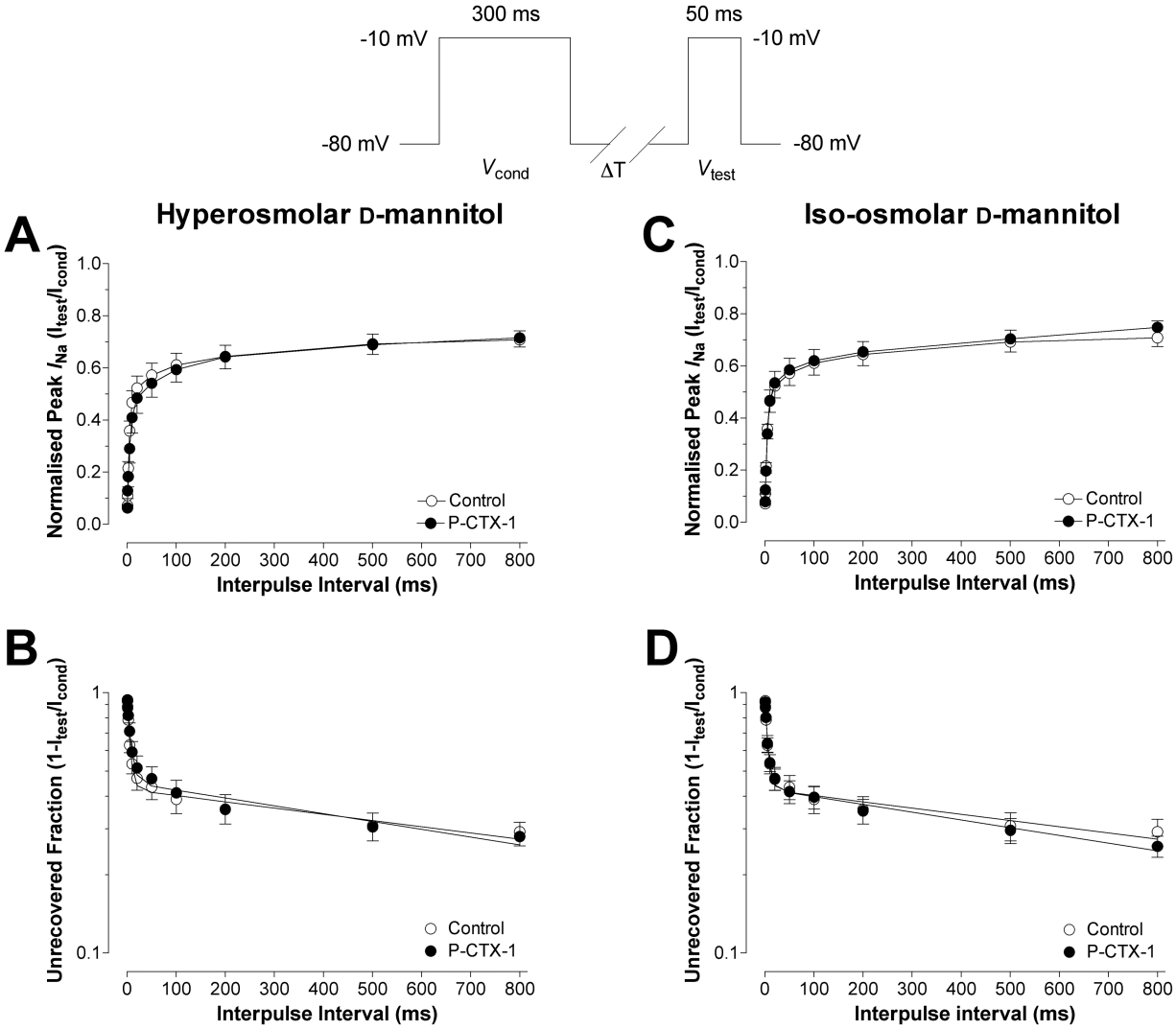

Fig. 7. Effects of D-mannitol on the P-CTX-1-induced increase in TTX-resistant Na_v channel repriming kinetics. The rate of recovery from inactivation was assessed using a standard two-pulse protocol (see *inset*), where ΔT represents a variable interpulse interval. Na_v channel repriming rate was determined by normalising peak I_{Na} elicited during the test pulse (V_{test}) against peak currents recorded during the conditioning pulse (V_{cond}) and plotted as a function of the interpulse interval.

(A-D) TTX-Resistant I_{Na} were recorded under control conditions (○), and following a 10 min perfusion with 5 nM P-CTX-1 (●) in the presence of hyperosmolar (A-B), or iso-osmolar (C-D), 50 mM D-mannitol. (B, D) The magnitude of the unrecovered fraction of current was plotted on a semilogarithmic scale. Data were fitted to the sum of two exponential functions according to equation 3, $n \geq 4$ for all experiments.